

SCION: Size-aware Policy Orchestration for Nonstationary Object Caches (Long Paper Version)

Qizhi Wang
PingCAP, Data & AI-Innovation Lab
Beijing, China
qizhi.wang@pingcap.com

Abstract

Object caches underpin modern cloud and edge services (CDNs, object stores, and large-scale web/KV caching), yet production workloads are heterogeneous, nonstationary, and throughput-constrained. Recent strong non-ML policies (e.g., SIEVE and S3-FIFO) raise the bar for any learned approach: added intelligence must be overhead-aware, robust under drift, and competitive with strong baselines. We present SCION, a lightweight *policy-orchestration* framework that selects among a small set of deployable cache policies using a tiny workload fingerprint computed off the critical path. Our prototype instance, AUTO, computes a short-prefix fingerprint (log p50/p90/mean object size, log tail ratio, cacheable fraction, unique ratio, and log cache size; default $N=200k$) and uses a linear selector trained offline with leave-one-trace-out validation to choose among GDSF, S3-FIFO, SIEVE, LHD, W-TinyLFU-AV, and DynamicAdaptiveClimb; a simpler SCION-P90 variant uses only a p90 threshold. Using a CPU-only, trace-driven evaluation built on `libCacheSim` and 30 public object-cache traces from `cache_dataset` (5M requests each, plus 20M for four long traces), and a separate HR-Cache (hazard-rate cache) simulator on a 10-trace subset, AUTO improves cacheable-only object miss ratio (OMR) over SIEVE on a majority of workloads, stays close to the best single expert on average (GDSF remains the best average-OMR baseline), and enables explicit OMR/BMR tradeoff selection while remaining competitive on byte miss ratio (BMR). Under a fast-policy budget, AUTO-FAST achieves a lower $\alpha=0.5$ cost than the best fixed fast policy. We quantify prefix-selection stability over post-prefix windows, fingerprint cost, and per-policy throughput overheads, and release a fully reproducible benchmark pipeline. SCION operationalizes a learning-lite orchestration design point that reduces regime-mismatch risk while keeping the hot path unchanged.

1 Introduction

Object caches are ubiquitous in future-generation computing systems (CDNs, cloud object stores, web caches, and key-value (KV) caching layers) and operate under strict throughput and latency constraints. Unlike CPU caches, object sizes are heavy-tailed and misses have non-uniform costs; a miss on a large object can dominate backend bandwidth, tail latency, and cross-region traffic. As a result, byte miss ratio (BMR) is often a primary operator metric alongside OMR. Workloads also drift with diurnal patterns, multi-tenancy, and shifting content mixes. Recent systems work has introduced simple yet strong policies, notably SIEVE and S3-FIFO, that raise the baseline for any learned approach [28, 26].

Problem. Production caches face *heterogeneous* and *nonstationary* workloads. Even strong policies exhibit regime-specific weaknesses: a policy that excels for KB-scale objects can degrade under MB-scale objects (and vice versa). This makes “pick one policy” risky—in our traces, the wrong choice can increase cacheable-only OMR by > 0.2 on some workloads—but also suggests a pragmatic opportunity: if workloads can be fingerprinted cheaply, then *choosing the right strong policy* can outperform any fixed choice without heavy per-request ML.

Motivation. Operators rarely deploy heavyweight ML on the hot path, but they do switch policies across tiers or services. The gap is *automation with low overhead*: a selector that is cheap enough to run outside the per-request path, yet accurate enough to avoid catastrophic regime mismatch. SCION targets this point in the design space.

Thesis and approach. The current frontier in learned caching is moving away from heavy per-request inference toward minimal-overhead, robust, deployable designs [19, 16, 20, 23, 29]. We adopt this perspective and propose SCION, a learning-lite orchestration layer: use a tiny fingerprint (computed rarely) to select among

a small set of expert policies (implemented with existing, battle-tested logic). The serving path remains purely “systems code”; learning/inference is off the critical path. When the selector is uncertain, we fall back to a conservative expert (GDSF by default for OMR), and quantify fallback sensitivity in Table 11. Figure 1 summarizes the deployment model: a lightweight off-path selector chooses one expert from a small portfolio using a short-prefix workload fingerprint, while the request path remains a single active expert cache.

Terminology and notation. We consider a cache of capacity C bytes serving requests for objects of size s . The *per-request path* is the hot path that executes admission and eviction for each request. *Off-critical-path inference* refers to computations performed outside that path (e.g., once per N -request epoch). We report object miss ratio (OMR) and byte miss ratio (BMR); *cacheable-only* metrics restrict to requests with $s \leq C$. N denotes the prefix/window length used for fingerprinting; τ is the p90 threshold in SCION-P90; p90 is the 90th percentile of object size in the prefix. Let $x \in \mathbb{R}^d$ be the fingerprint feature vector with $d=7$ features (log p50/p90/mean size, log tail ratio, cacheable fraction, unique ratio, log cache size), where the *unique ratio* is the fraction of distinct object IDs in the prefix (1–reuse). SCION is the framework; AUTO is its default learned selector instance.

Contributions.

- **Learning-lite orchestration.** A lightweight policy-orchestration abstraction with a reject-option fallback: small action space, cheap fingerprints, and strong baselines as experts (section 3).
- **A minimal instance.** AUTO uses a tiny multi-feature fingerprint (log p50/p90/mean size, log tail ratio, cacheability, unique ratio, cache size) and a linear selector (trained via leave-one-trace-out) to choose among six strong experts; a simple SCION-P90 threshold is an ablation (section 3.2).
- **Reproducible evaluation.** A CPU-only, trace-driven benchmark and scripts based on `libCacheSim` [24] and 30 public traces from `cache_dataset` [25], with bootstrap confidence intervals and trace integrity diagnostics (section 4).
- **Robustness analysis.** Sensitivity studies over (N, τ) and fingerprints, prefix-stability analysis over post-prefix windows, out-of-distribution generalization across dataset families, spliced-trace nonstationarity tests with hysteresis and bandit baselines, plus worst-5% window tail analysis (section 5).
- **Overhead accounting.** Microbenchmarks for fingerprint cost and per-policy throughput, plus a separate

HR-Cache baseline evaluated on an overlapping subset (section 5).

- **Engineering and artifact.** We integrate `DynamicAdaptiveClimb` into `libCacheSim`, build a trace-conversion and evaluation pipeline for HR-Cache, and provide end-to-end scripts to download traces, run all experiments, and regenerate tables/figures. We surface key per-workload wins and CIs in the paper, while full per-workload, spliced-trace, and tradeoff example tables are included in the artifact to keep the paper concise.
- **Operational relevance.** AUTO improves cacheable-only OMR over SIEVE on most workloads, matches or exceeds the best expert on small-object regimes, and supports explicit OMR/BMR tradeoffs useful to cloud and edge operators (section 5).

2 Background and Motivation

Object caching and size effects. Object caches must decide (i) whether to admit an object on a miss and (ii) what to evict when space is needed. Because objects vary widely in size, a policy that ignores size may suffer from pollution and poor byte efficiency. Classic approaches include TinyLFU-style admission [9] and size-aware scoring such as the GreedyDual-Size family (GDS/GDSF) [5].

The new baseline reality. SIEVE and S3-FIFO show that simple mechanisms can be highly competitive in object caches [28, 26]. This shifts what is publishable: “ML beats LRU” is no longer interesting; the bar is beating strong non-ML baselines *and* accounting for overhead and robustness.

Why orchestration. Many deployments already swap policies across tiers or services; however, manual selection is brittle under workload drift. An orchestration layer can automate selection while keeping the per-request path simple. This idea echoes mixture-of-experts in caching (e.g., Cacheus) [16] and minimal-overhead learned methods [23], and online expert tracking (e.g., LeCaR-style) but here we focus on an especially constrained, reproducible design point: a tiny fingerprint and a tiny expert set. Learning is confined to offline selector training; at runtime, the cache executes a standard expert policy with no per-request ML.

3 SCION Method

SCION defines the orchestration abstraction; AUTO is its default instantiation with a learned linear selector.

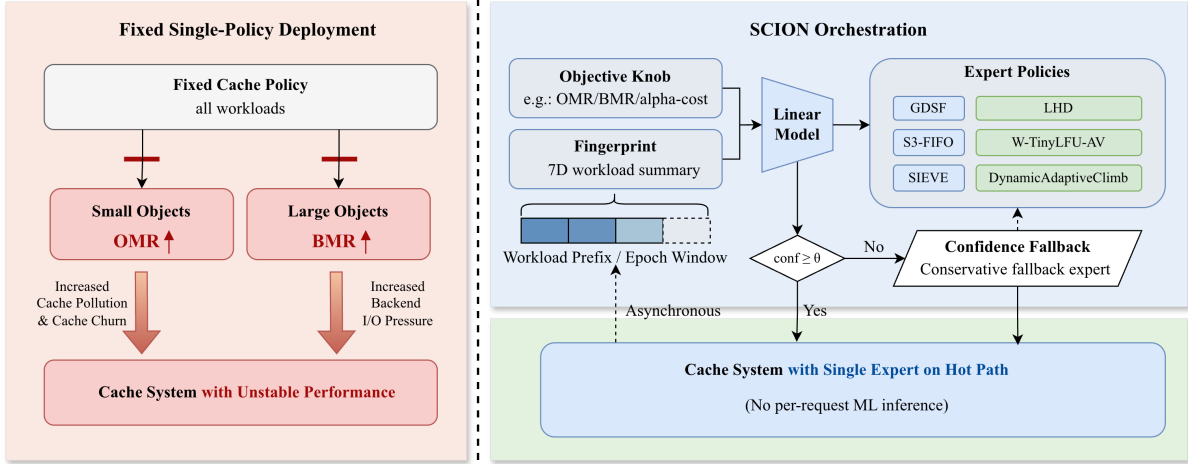


Figure 1: SCION architecture. A lightweight off-path selector chooses one expert from a small portfolio using a short-prefix workload fingerprint, while the request path remains a single active expert cache with standard hit/miss handling.

3.1 Design principles

SCION selects among experts $\mathcal{E} = \{e_1, \dots, e_k\}$. We design for:

- **Tiny action space.** Keep k small and experts strong (e.g., SIEVE, S3-FIFO, GDSF, W-TinyLFU, LHD, AdaptiveClimb/DynamicAdaptiveClimb).
- **Cheap fingerprint.** Use statistics computable on a short prefix or a short window.
- **Off-critical-path inference.** Selection runs infrequently (per epoch/window), not per request.
- **Robustness-first framing.** When the selector is unsure, matching a strong baseline is acceptable; correctness is defined by avoiding catastrophic regime mismatch.
- **Safe fallback.** Low-confidence decisions trigger a conservative expert, and epochal selection can include hysteresis/lag to reduce oscillation.

3.2 A minimal instance: AUTO

Our default instance uses a tiny multi-feature fingerprint computed on the first N requests of a trace or window: $\log p50$, $\log p90$, \log mean object size, \log tail ratio ($p90/p50$), cacheable fraction at the target cache size, unique ratio (distinct IDs divided by N), and \log cache size. The cacheable fraction is computed from the prefix alone as the fraction of prefix requests with object size $s \leq C$ (no lookahead beyond the prefix). In production, cacheable and unique ratios can be estimated with approximate distinct counters (e.g., HyperLogLog) without changing the regime-level decision. Let $x \in \mathbb{R}^d$ be this

feature vector with $d=7$. For each expert $e \in \mathcal{E}$, we learn a linear score $s_e = w_e^\top x$ and select

$$\pi(x) = \arg \max_{e \in \mathcal{E}} s_e.$$

Objective view. For each sample i and expert e , let $\ell_i(e)$ be the objective value (OMR, BMR, or α -cost), and define regret $r_i(e) = \ell_i(e) - \min_{e'} \ell_i(e')$. Learning a linear selector is thus a lightweight, cost-sensitive classification problem; lower misclassification implies lower expected regret, and we report regret directly. The confidence threshold implements a *reject option*: if $\max_e p(e | x) < \theta$ we abstain and fall back to a conservative expert, yielding a simple risk-coverage tradeoff that we tune on training folds. With fallback expert e_0 and indicator $A = \mathbb{1}[\max_e p(e | x) \geq \theta]$, the expected regret decomposes as $\mathbb{E}[r_i(\hat{e})A + r_i(e_0)(1 - A)]$ and is bounded by $\mathbb{E}[\Delta_i \mathbb{1}[\hat{e} \neq e^*]] + \mathbb{E}[r_i(e_0)(1 - A)]$, where Δ_i is the per-sample expert spread and e^* the best expert. We train w_e with leave-one-trace-out validation on trace-size pairs; labels use full-run best-expert on the training fold only, and all normalization/tuning is fold-local (no held-out leakage). Samples are weighted uniformly across pairs (no per-trace reweighting); because each trace contributes the same four cache sizes after filtering, this is equivalent to per-trace weighting (artifact). At inference time, selection is a single dot product per expert, performed once per epoch (not per request). If the classifier confidence is low, we fall back to a conservative expert (by default, the best-average policy).

Confidence and fallback. We compute confidence as the maximum softmax probability of the linear classifier. If $\max_e p(e | x) < 0.40$, we fall back to the best-average

expert on the training fold for the *same objective* (unless a fixed fallback is specified), so BMR-centric selectors default to a BMR-optimized fallback. Table 11 shows that, on this suite, GDSF minimizes average and tail regret for both OMR and $\alpha=0.2$ while other fallbacks increase regret modestly; we therefore keep GDSF as the default in our experiments. Under the fast-policy budget (Table 24), the fallback shifts to the best-average fast policy (typically LHD). For online selection on spliced traces, we apply minimal hysteresis (min-stay of one window) and a one-window lag to avoid reacting to intra-window noise.

A simple ablation: SCION-P90. For comparison, we include a single-statistic selector using the prefix p90 size:

$$\pi(p90) = \begin{cases} \text{GDSF}, & p90 \geq \tau \\ \text{S3-FIFO}, & p90 < \tau \end{cases}$$

Here p90 is the 90th percentile of object size in the prefix and τ is a size threshold (bytes). This mirrors the original mean-threshold intuition but is more robust under heavy tails.

Default hyperparameters. Unless otherwise stated, we fix $N=200k$, window size 200k, and use leave-one-trace-out tuning for τ in SCION-P90 over a small grid of thresholds. In our evaluation, the expert set includes GDSF, S3-FIFO, SIEVE, LHD, WTinyLFU-AV, and DynamicAdaptiveClimb. We also evaluate AdaptiveClimb as an additional baseline. We train separate selectors per objective; AUTO targets OMR by default, while cost-weighted objectives use their own selectors.

Selector training details. The selector is trained offline to map fingerprints to the best expert under each objective, using held-out traces for validation. We train a multinomial (softmax) linear classifier per objective on standardized features (z-scored per fold), using batch gradient descent (800 steps, learning rate 0.1) with L_2 regularization (10^{-3}), and no per-trace reweighting. Labels are the best-performing expert for each trace-size sample under the objective. If multiple experts tie within 10^{-6} , we mark the sample as *flat* (degenerate) for analysis; label ties are broken deterministically by CSV order. For leave-one-trace-out, each sample’s fallback policy is the best-average expert on the corresponding training fold.

Overhead. The fingerprint requires parsing only N records once per trace/epoch. All per-request logic is inherited from the chosen expert. This aligns with the minimal-overhead direction in recent learned caching work [23, 29].

4 Experimental Setup

Simulator and implementation. We implement a trace-driven benchmark in C++ on top of libCacheSim [24]. Experiments are CPU-only and generate CSV outputs, summary tables, and PDF figures. Unless otherwise stated, AUTO makes a single selection using the first N requests of each trace and keeps that expert for the full run; only the spliced-trace experiments re-select at window boundaries with lag/min-stay.

Why CPU-only and trace-driven. “CPU-only” here refers to the evaluation platform (no GPU/ML acceleration), not the provenance of traces. Our traces come from CDN/object-cache workloads; trace-driven simulation provides reproducibility and isolates replacement effects, and we complement it with a lightweight HTTP prototype to sanity-check end-to-end behavior.

Engineering scope. Beyond the core selector, we integrated AdaptiveClimb/DynamicAdaptiveClimb into libCacheSim, built a trace conversion pipeline to evaluate HR-Cache with matched windows, and implemented end-to-end scripts for trace download, experiment sweeps, spliced-trace generation, overhead measurement, and paper asset export.

Traces. We use 30 public object-cache traces from `cache_dataset` [25] (oracleGeneral format), spanning Meta CDN workloads (reag/rprn/rnha), Wikipedia 2019, 10 Twitter clusters, Alibaba/Tencent block caches, CloudPhysics traces, MSR traces, and Meta KV. For broad coverage we cap each run at 5M requests and sweep cache sizes {128, 256, 512, 1024} MiB. For four long traces (`meta_reag`, `meta_rprn`, `wiki_2019t`, `twitter_cluster10`) we additionally run 20M requests to check stability. Table 1 summarizes prefix statistics and cacheability/uniqueness diagnostics.

Data diagnostics and anomalies. We do not alter the public traces; instead, we surface diagnostics (prefix size percentiles, cacheable and unique ratios, and per-trace OMR ranges across policies) and flag trace-size pairs where policies are indistinguishable (OMR range $\leq 10^{-6}$) as degenerate. These flagged pairs are excluded from win-count statistics but retained in summary averages for transparency. Some Twitter clusters contain zero-size records in the public dataset, which leads to 0-valued percentiles in Table 1; we keep these entries and rely on the diagnostics to identify their impact. Because SCION uses percentile- and tail-based features (not means), isolated zero-size records primarily affect the lower tail and have limited influence on p90-based fingerprints. When percentiles are zero (a few Twitter clusters), we flag those trace-size pairs as degenerate for

Table 1: Prefix trace diagnostics (size percentiles, cacheable and unique ratios). Sizes are in KiB/MiB; a few Twitter clusters include zero-size records in the public traces, which yields 0-sized percentiles and are flagged as degenerate for win-count statistics.

Trace	p50	p90	Mean	Cacheable	Unique
Alibaba-0	4.0KiB	420.0KiB	69.9KiB	1.000	0.439
Alibaba-1	4.0KiB	8.0KiB	6.2KiB	1.000	0.159
Alibaba-100	8.0KiB	28.0KiB	12.0KiB	1.000	0.935
Alibaba-103	12.0KiB	72.0KiB	29.5KiB	1.000	0.778
Alibaba-11	8.0KiB	32.0KiB	15.7KiB	1.000	0.680
Alibaba-12	8.0KiB	504.0KiB	89.4KiB	1.000	0.984
Meta-KV-1	0.1KiB	0.4KiB	0.5KiB	1.000	0.180
Meta-reag	26.8KiB	8.2MiB	23.0MiB	0.989	0.428
Meta-rnha	64.6KiB	20.1MiB	41.0MiB	0.985	0.688
Meta-rprn	55.7KiB	10.0MiB	32.3MiB	0.992	0.575
MSR-prn-0	4.0KiB	64.0KiB	14.1KiB	1.000	0.395
MSR-prj-0	4.0KiB	64.0KiB	14.0KiB	1.000	0.268
MSR-prxy-0	1.0KiB	4.0KiB	2.8KiB	1.000	0.054
Tencent-10000	4.0KiB	12.0KiB	8.7KiB	1.000	0.290
Tencent-10001	4.0KiB	112.0KiB	22.5KiB	1.000	0.745
Tencent-10100	4.0KiB	32.0KiB	20.7KiB	1.000	0.626
Tencent-10348	4.0KiB	40.0KiB	18.8KiB	1.000	0.384
Tencent-10512	4.0KiB	32.0KiB	18.4KiB	1.000	0.629
Tencent-10533	4.0KiB	48.0KiB	17.7KiB	1.000	0.085
Twitter-10	0.0KiB	0.0KiB	0.0KiB	1.000	0.500
Twitter-13	0.0KiB	3.8KiB	2.3KiB	1.000	0.629
Twitter-20	0.1KiB	0.1KiB	0.1KiB	1.000	0.139
Twitter-26	0.1KiB	0.2KiB	0.2KiB	1.000	0.077
Twitter-3	0.1KiB	0.3KiB	0.2KiB	1.000	0.075
Twitter-35	0.0KiB	5.0KiB	1.3KiB	1.000	0.077
CloudPhysics-w01	3.5KiB	6.5KiB	16.1KiB	1.000	0.870
CloudPhysics-w02	16.0KiB	128.0KiB	47.8KiB	1.000	0.335
CloudPhysics-w03	32.0KiB	256.0KiB	71.6KiB	1.000	0.608
CloudPhysics-w04	32.0KiB	256.0KiB	79.9KiB	1.000	0.493
Wiki-2019t	22.0KiB	70.4KiB	33.3KiB	1.000	0.707

win-count statistics; the zeros remain visible in the diagnostics and in the selector’s input features. Removing the three zero-size Twitter clusters (Twitter-10/13/35) shifts mean cacheable-only OMR by +0.0039 for AUTO and +0.0036 for GDSF, and does not change the policy ordering (artifact).

Metrics and “cacheable-only” reporting. Traces can contain objects larger than the cache capacity; those requests are effectively uncacheable and can distort conclusions. We report cacheable-only object miss ratio (OMR) and cacheable-only byte miss ratio (BMR), computed over requests/bytes restricted to objects whose size fits within the evaluated cache capacity. We also report all-request OMR/BMR (including uncacheable objects) for operational interpretation. OMR is a proxy for hit ratio and user-facing latency, while BMR captures backend bandwidth and cost; in object caches, large objects can dominate bytes even when OMR is low, so we report both. We compute bootstrap confidence intervals (CIs) from windowed miss ratios, and report trace integrity statistics (size percentiles, cacheable ratio, unique ratio) to identify degenerate trace-size pairs. Because cacheable-only and all-request objectives can diverge, we include concrete tradeoff examples in the reproducibility artifact.

Compared policies. We report AUTO (selector over {GDSF, S3-FIFO, SIEVE, LHD, W-TinyLFU-AV, DynamicAdaptiveClimb [3]}) and its experts, and compare against additional baselines including AdaptiveClimb [3],

W-TinyLFU, AdaptSize-style admission (admit with probability $\exp(-\text{size}/C)$; we tune C with a small grid per trace), and classic policies such as ARC, TwoQ, LIRS, LeCaR, and Cacheus (supported by our benchmark harness). We also evaluate HR-Cache (hazard-rate cache) [21] using its open-source simulator on a 10-trace subset and two cache sizes (256/1024 MiB), converting traces to its input format (32-bit ids/sizes) and matching our 200k-window evaluation cadence.

System prototype. To validate feasibility beyond trace-driven simulation, we implement a lightweight end-to-end prototype: an in-memory cache daemon (this work) serves HTTP GET requests and fetches misses from a local origin server, with optional TTLs but no revalidation logic. The daemon uses the same policy logic as the simulator (GDSF, S3-FIFO, SIEVE, and AUTO), and exposes hit ratio and origin byte counters. We replay a smaller prefix of each trace to keep the run time reasonable and report latency, throughput, and resource usage. We optionally inject origin-side delay to emulate network jitter. For the prototype, AUTO uses the p90-threshold selector (SCION-P90) to avoid offline training dependencies. Unless otherwise stated, the prototype uses a 256 MiB cache, replays 20k requests per trace, and issues concurrent GETs with client concurrency 128. This prototype omits revalidation, invalidations, and distributed cache behavior; it is intended as a feasibility check rather than a production model.

5 Results

5.1 Aggregate performance

Table 3 summarizes average cacheable-only miss ratios. Across workloads, AUTO is competitive with the strongest experts on OMR while reducing the risk of regime mismatch; its average OMR remains close to the best-performing expert, but avoids large mismatches when the workload falls into a different regime. GDSF remains the strongest average-OMR baseline on this suite. We compute 95% bootstrap confidence intervals (CIs) over trace-size pairs for key policies and report them in Table 3, highlighting that the observed differences are often small but consistent. All-request averages show the same ordering: AUTO OMR/BMR 0.439/0.575 versus GDSF 0.433/0.577 and SIEVE 0.479/0.596, and Table 15 summarizes cacheable-only OMR vs all-request BMR tradeoffs. Against GDSF, we do not observe the specific conflict “better cacheable-only OMR but worse all-request BMR”; operationally, the usual tradeoff is instead slightly higher OMR for slightly lower BMR.

Fast-policy budget as a primary operating point. For CPU-constrained deployments we treat the fast-

policy budget as a primary operating point (not just a side analysis). The fast set excludes WTinyLFU-AV because its single-threaded throughput is $< 1\%$ of SIEVE in our implementation, so fast-policy conclusions are not driven by that outlier. Production TinyLFU variants (e.g., Caffeine/Ristretto) and cost-aware GDS approximations are not yet available in our simulator; they are natural fast-policy additions for future SCION deployments. Table 24 reports AUTO-FAST against the best fixed fast policy and the fast-set oracle; AUTO-FAST trades a small OMR increase for a larger BMR reduction, yielding a lower $\alpha=0.5$ cost than the fixed fast baseline.

Why OMR improves. On large-object regimes, size-aware experts reduce object misses among cacheable objects, while FIFO-family designs can be misled by object-size heterogeneity. On small-object regimes, S3-FIFO is already near-optimal among our compared baselines; SCION simply selects it, avoiding degradation.

Case studies (with CIs). Example (CloudPhysics-w02, 1 GiB): AUTO selects GDSF, achieving cacheable-only OMR 0.438 [0.428, 0.454] versus SIEVE 0.976 [0.971, 0.981], and BMR 0.888 vs 0.995 (10.7 percentage points lower). Example (Alibaba-103, 256 MiB): AUTO selects WTinyLFU-AV, achieving cacheable-only OMR 0.768 [0.758, 0.784] versus GDSF 0.823 [0.814, 0.835], and BMR 0.872 vs 0.914. More per-trace examples are in the reproducibility artifact.

Table 2: Representative per-trace examples with OMR CIs (AUTO vs baseline).

Trace	Cache	AUTO policy	AUTO OMR [CI]	Baseline	Baseline OMR [CI]
CloudPhysics-w02	1GiB	GDSF	0.438 [0.428,0.454]	SIEVE	0.976 [0.971,0.981]
Alibaba-103	256MiB	WTinyLFU-AV	0.768 [0.758,0.784]	GDSF	0.823 [0.814,0.835]
CloudPhysics-w02	128MiB	GDSF	0.979 [0.975,0.984]	WTinyLFU-AV	0.734 [0.714,0.758]

Table 3: Average cacheable-only miss ratios over all evaluated workloads with 95% bootstrap CIs. Lower is better.

Policy	Avg OMR (95% CI)	Avg BMR (95% CI)
AUTO	0.438240 [0.388795,0.490928]	0.528066 [0.469773,0.586067]
SIEVE	0.479133 [0.423313,0.532635]	0.541692 [0.484306,0.600559]
S3-FIFO	0.468178 [0.413922,0.521532]	0.566012 [0.511392,0.624286]
GDSF	0.432585 [0.381961,0.484499]	0.530435 [0.471803,0.588821]
DynamicAdaptiveClimb	0.470352 [0.415332,0.524424]	0.532683 [0.473753,0.592131]

Per-family summary. Table 4 aggregates cacheable-only OMR by dataset family (averaged over trace-size pairs with bootstrap CIs), surfacing consistent regime differences across families. We report AUTO, a size-aware baseline (GDSF), and a FIFO-family baseline (S3-FIFO); full per-trace results remain in the artifact. Figure 2 provides the same comparison visually and makes the regime split across families easier to scan.

Table 4: Family-level cacheable-only OMR summary (95% CIs).

Family	N	AUTO	GDSF	S3-FIFO
Block	48	0.448 [0.378,0.514]	0.444 [0.372,0.518]	0.480 [0.410,0.551]
CloudPhysics	16	0.726 [0.643,0.799]	0.696 [0.633,0.758]	0.801 [0.733,0.869]
MSR	12	0.189 [0.110,0.281]	0.189 [0.110,0.277]	0.209 [0.134,0.291]
Meta-CDN	12	0.654 [0.585,0.714]	0.654 [0.585,0.717]	0.704 [0.640,0.766]
Meta-KV	4	0.151 [0.141,0.164]	0.141 [0.141,0.142]	0.151 [0.141,0.165]
Twitter	24	0.236 [0.137,0.330]	0.235 [0.153,0.325]	0.235 [0.148,0.333]
Wiki	4	0.771 [0.689,0.843]	0.793 [0.726,0.847]	0.775 [0.717,0.840]

AUTO vs strong baselines. Table 5 summarizes AUTO-baseline OMR deltas (negative favors AUTO). Averaged over all trace-size pairs, AUTO improves S3-FIFO on 65.8% of pairs (avg $\Delta = -0.0299$) and improves GDSF on 13.3% of pairs (avg $\Delta = +0.0057$), illustrating the regime-mismatch tradeoff with a very strong size-aware baseline. Against GDSF, 72/120 pairs are ties. Family-wise, AUTO is best on Wiki ($\Delta\text{OMR} -0.0215$, $\Delta\text{BMR} -0.0468$), roughly tied on Meta/Twitter/MSR, and most clearly loses on CloudPhysics ($\Delta\text{OMR} +0.0299$), where a single expert dominates across sizes; block traces sit in between with a small average OMR loss (+0.0044) but average BMR gain (-0.0062). The largest overall AUTO gaps occur on CloudPhysics w02/w01 (avg gaps 0.133/0.130; max gaps 0.246/0.153), so these are natural “pin GDSF” regimes.

Table 5: Key aggregate gains vs strong baselines on cacheable-only OMR (delta = AUTO - baseline).

Baseline	Improve%	Avg Δ	Best Δ	Worst Δ
GDSF	13.3	0.0057	-0.2030	0.1402
S3-FIFO	65.8	-0.0299	-0.5426	0.0841

CI computation bootstraps the per trace-size averages (500 resamples) rather than individual requests/windows,

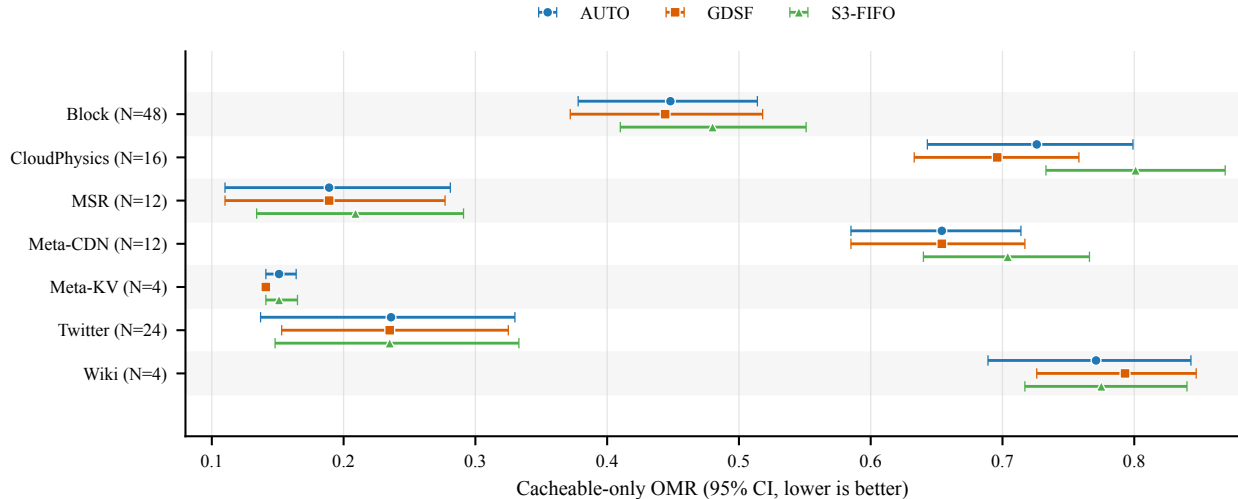


Figure 2: Family-level cacheable-only OMR with 95% CIs. The regime split is stable across families: CloudPhysics favors GDSF, Wiki favors AUTO, and FIFO-family policies trail on the large-object families.

preserving within-trace dependence by treating each trace-size pair as the resampling unit.

SCION-P90 ablation. SCION-P90 (artifact table) is competitive but trails AUTO on average OMR/BMR across all trace-size pairs. AUTO reduces cacheable-only OMR by ≈ 0.020 and BMR by ≈ 0.006 relative to SCION-P90, indicating that the multi-feature selector adds value beyond a single threshold. SCION-P90 matches AUTO on 21.7% of pairs overall; because SCION-P90 can only choose between GDSF and S3-FIFO, it matches AUTO on 48.1% of the pairs where AUTO selects one of those two experts (artifact). AUTO helps most when p_{90} is near τ (artifact), where cacheability/uniqueness features provide additional separation (table 12).

HR-Cache subset. Table 9 compares HR-Cache [21] against our baselines on the overlapping subset (10 traces, 256/1024 MiB). HR-Cache achieves competitive BMR on this subset; the BMR-aligned selector $\text{AUTO}(\alpha=0.2)$ closes much of the gap, while AUTO and our strongest non-ML baselines remain strong on OMR. HR-Cache expects 32-bit signed IDs/sizes; our conversion maps IDs via modulo and clamps sizes to that range, which can introduce collisions. Accordingly, we treat HR-Cache results as a cross-check rather than a definitive head-to-head ranking. The subset reflects the extra conversion/build steps required by the HR-Cache simulator; we provide scripts to extend it further.

Classic baselines. Table 6 reports ARC and TwoQ on a 6-trace subset (smallest HR-Cache traces, 256/1024 MiB), using the first 20k requests per trace to keep runtime manageable for these heavier policies.

LIRS is substantially slower in our simulator (minutes per 20k requests on mid-sized traces), so we report it on the two smallest traces using 5k-request prefixes; the table includes per-policy sample counts (N). These classical policies are effectively tied on this small subset; because the prefixes are much shorter than the main suite, these values are not directly comparable to full-suite averages and are intended as qualitative anchors. We do not see evidence that they dominate the best size-aware experts on cacheable-only OMR.

Table 6: Classic baselines on a small HR-Cache subset (cacheable-only averages; 20k-request prefixes for ARC/TwoQ, 5k for LIRS; N shows samples).

Policy	Avg OMR ↓	Avg BMR ↓	N
ARC	0.382226	0.448056	12
TwoQ	0.379894	0.472687	12
LIRS	0.422354	0.529858	4

Learned baselines subset. To position against learned baselines, we evaluate LeCaR, Cacheus, and LRB-BMR (LightGBM-based learned replacement optimizing BMR) on the 10-trace subset using 200k requests and four cache sizes (128/256/512/1024 MiB). Table 7 shows that LeCaR attains the best average OMR on the successful 32-pair subset (0.504), while the BMR-oriented selector $\text{AUTO}(\alpha=0.2)$ achieves the lowest average BMR in our harness (0.466 vs 0.472 for LRB-BMR) with lower average OMR than LRB-BMR (0.520 vs 0.530). Default AUTO remains close to GDSF on OMR (0.513 vs 0.510), illustrating that SCION’s value

is exposing explicit operating points rather than dominating every specialized learned baseline on its home objective. This limited subset is meant as a qualitative anchor rather than a full-suite comparison; full results and scripts are in the artifact.

Table 7: Learned baselines on the 10-trace subset (cacheable-only averages; 200k requests; 128/256/512/1024 MiB).

Policy	Avg OMR ↓	Avg BMR ↓	N
AUTO	0.513082	0.496279	40
AUTO ($\alpha = 0.2$)	0.520135	0.465623	40
GDSF	0.510144	0.507296	40
LeCaR	0.504318	0.507363	32
Cacheus	0.526992	0.482302	40
LRB-BMR	0.529727	0.471793	40

Oracle lookahead bounds. To contextualize headroom, we also report oracle lookahead policies (Belady and BeladySize) on a 6-trace subset using 20k-request prefixes (oracleGeneral traces include next-access timestamps). Table 8 provides cacheable-only averages; these act as lightweight object- and size-aware lower bounds. On this subset, BeladySize reaches 0.372 OMR / 0.447 BMR, versus 0.375 / 0.466 for the strongest online expert (GDSF), so the residual gap is modest for OMR but clearer for byte-oriented objectives. Belady lowers OMR further (0.346) while worsening BMR relative to BeladySize, reinforcing that object-optimal and byte-aware offline comparators differ under variable sizes. Tighter flow-based bounds such as FOO/PFOO are therefore complementary [4], but require a different harness, so we leave them for future work.

Table 8: Oracle lookahead bounds on a small subset (cacheable-only averages; 20k-request prefixes).

Policy	Avg OMR ↓	Avg BMR ↓
Belady	0.377158	0.445614
BeladySize	0.372115	0.447127

Selector accuracy. Table 10 reports leave-one-trace-out selector accuracy and regret distributions. We define *regret* as the per-sample objective gap between the selected policy and the best expert (e.g., $\text{OMR}_{\text{chosen}} - \min_e \text{OMR}_e$), and mark a sample as *nonflat* if the best-worst gap exceeds 10^{-6} . The selector is accurate on non-degenerate trace-size pairs and exhibits low average regret. Per-trace avg regret has median 0.0079 and P90 0.0675; per-trace p90-regret median 0.0126 (P90 0.1003)

Table 9: Average cacheable-only miss ratios on the HR-Cache subset.

Policy	Avg OMR ↓	Avg BMR ↓
HR-Cache	0.504266	0.457858
AUTO ($\alpha = 0.2$)	0.490309	0.452126
AUTO	0.483891	0.482311
SIEVE	0.508924	0.450670
S3-FIFO	0.502109	0.558957
GDSF	0.475218	0.487148
DynamicAdaptiveClimb	0.499772	0.435142

(artifact), indicating most traces are low-regret with a small tail of difficult cases. Low-confidence triggers are concentrated in a few traces (artifact); Table 10 reports low-confidence fractions by objective, with 16.3% of non-flat OMR pairs falling back in the final AUTO setting (leave-one-trace-out). Top-1 calibration on non-flat OMR samples yields ECE 0.10 and Brier 0.21, indicating mild overconfidence; temperature scaling does not improve regret (artifact). A threshold sweep in the 6-expert sensitivity study shows the coverage-regret tradeoff and motivates $\theta=0.40$ (artifact).

Table 10: Selector accuracy and regret (lower regret is better).

Objective	Subset	Acc	Avg regret	P95 regret	Worst regret	Low-conf%
cost:0.2	all	0.433	0.024102	0.113755	0.182123	42.5
cost:0.2	nonflat	0.327	0.029513	0.116286	0.182123	51.0
cost:0.5	all	0.508	0.020515	0.106438	0.189169	42.5
cost:0.5	nonflat	0.418	0.025121	0.109354	0.189169	51.0
cost:0.8	all	0.558	0.015684	0.096900	0.203912	16.7
cost:0.8	nonflat	0.500	0.019205	0.106430	0.203912	17.3
omr	all	0.525	0.019668	0.110751	0.245795	14.2
omr	nonflat	0.459	0.024084	0.119545	0.245795	16.3

Model sensitivity. We compare the linear softmax selector (standardized features) to an unstandardized variant and a tiny one-hidden-layer MLP. Model sensitivity results are reported in the reproducibility artifact; standardization matters for linear models, and a tiny MLP slightly improves average regret while increasing tail regret, so we keep the linear model for stability.

Selector ablations and fallback behavior. Table 12 drops one feature at a time; cacheability, uniqueness, and cache size contribute the largest regret increases, while p50/p90/mean/tail-ratio are comparatively redundant on this trace suite. A sweep over confidence thresholds (artifact) selects $\theta=0.40$; average regret varies by

< 0.005 across $\theta \in [0.3, 0.6]$. Temperature scaling does not change coverage or regret at $\theta=0.40$, so we report uncalibrated scores. Perturbing cacheable/unique ratios by 2–30% relative noise increases average regret by only 0.002–0.003 (artifact), consistent with sketching errors from HLL/t-digest-style estimators and showing headroom beyond typical 2–10% HLL-scale noise. We also report per-objective selector weights in the artifact; the largest coefficients align with cacheability/uniqueness and size percentiles, consistent with the regime split observed in the ablations. Table 11 summarizes objective-specific fallback sensitivity; richer uncertainty triggers are future work.

Table 11: Fallback sensitivity across objectives (non-flat samples; DynAdaptiveClimb = DynamicAdaptiveClimb).

Fallback	OMR avg	OMR P95	$\alpha=0.2$ avg	$\alpha=0.2$ P95
GDSF	0.0241	0.1195	0.0295	0.1163
DynAdaptiveClimb	0.0325	0.1218	0.0476	0.1627
LHD	0.0248	0.1195	0.0441	0.1638
S3-FIFO	0.0300	0.1277	0.0396	0.1401
SIEVE	0.0321	0.1277	0.0529	0.1884

Expert-set ablation. Table 13 drops one expert at a time and retrains the selector. We report the selector regret within the reduced set, the *oracle gap* (loss from removing an expert, relative to the full-set best), and the combined total gap. Dropping GDSF increases the oracle gap most, while LHD and WTinyLFU-AV also contribute non-trivial headroom in their regimes. Dropping WTinyLFU-AV changes the total gap only slightly (0.0152 vs 0.0158), indicating that conclusions are not driven by its slow implementation. Enumerating all 3- and 4-expert subsets (artifact) shows the best 4-expert subset has total gap 0.0130 and the best 3-expert subset has 0.0148, indicating modest loss when operators restrict implementations.

Error analysis. We bucket non-flat samples by feature quantiles (artifact). Misclassification rates are higher in small-object regimes (low p90) and low-unique-ratio regimes, while mid p90 bins exhibit lower regret, suggesting that additional reuse/burstiness features could further stabilize selection in small-object workloads. A lightweight reuse/burstiness sketch (e.g., a small count-min or recent-reuse histogram) is a plausible low-overhead extension.

Fallback frequency in practice. Using the actual AUTO selector (leave-one-trace-out, $\theta=0.40$), low-confidence cases account for 16.3% of non-flat trace-size

Table 12: Drop-one-feature ablation (non-flat samples).

Setting	Avg regret	Misclass rate
all	0.015819	0.367
drop log p50	0.016706	0.367
drop log p90	0.015819	0.367
drop log mean	0.015967	0.357
drop log tail ratio	0.016721	0.367
drop cacheable ratio	0.018268	0.367
drop unique ratio	0.018015	0.398
drop log cache size	0.018076	0.357

Table 13: Expert-set ablation (cacheable-only OMR).

Setting	Avg regret	Oracle gap	Total gap
all	0.0158	0.0000	0.0158
drop GDSF	0.0152	0.0098	0.0249
drop DynamicAdaptiveClimb	0.0178	0.0000	0.0178
drop LHD	0.0150	0.0021	0.0171
drop WTinyLFU-AV	0.0086	0.0066	0.0152
drop S3-FIFO	0.0145	0.0000	0.0145
drop SIEVE	0.0145	0.0000	0.0145

pairs, and all of those fall back to GDSF; nevertheless, AUTO selects a non-GDSF expert on 49.0% of non-flat pairs. Low-confidence fractions vary by family (MSR 0.36, block 0.21, CloudPhysics 0.12, and 0.0 for Meta-CDN/Twitter/Wiki); when fallback triggers, 68.8% of cases are within 0.01 regret and 87.5% within 0.02 (artifact).

OMR/BMR tradeoff. Table 14 shows average cost for $\alpha \in \{0.2, 0.5, 0.8\}$ in $\alpha \cdot \text{OMR} + (1 - \alpha) \cdot \text{BMR}$, demonstrating that SCION can explicitly target operator-weighted objectives. For example, $\text{AUTO}(\alpha=0.5)$ yields a slightly lower average cost than fixed GDSF (0.48126 vs 0.48151). We also summarize how often cacheable-only OMR improvements coincide with worse all-request BMR in Table 15. Case study (meta_rnha, 1 GiB): $\text{AUTO}(\alpha=0.2)$ selects DynamicAdaptiveClimb (OMR 0.784, all-request BMR 0.841), while $\text{AUTO}(\alpha=0.8)$ selects GDSF (OMR 0.737, all-request BMR 0.886), illustrating the operator-controlled tradeoff. Cross-objective robustness is reasonable: the $\alpha=0.5$ selector is within 0.0007 of the $\alpha=0.2$ -tuned cost and within 0.0035 of the $\alpha=0.8$ -tuned cost, suggesting modest sensitivity to operator weight drift. This supports a simple deployment strategy: pretrain a small set of selectors at a few α values and switch among them as preferences drift;

the $\alpha=0.2$ and $\alpha=0.8$ selectors choose different experts on 43.3% of trace-size pairs (artifact). Per-family and worst-case deltas for objective mismatch are included in the reproducibility artifact.

Table 14: Avg. cost tradeoff for α -weighted objective. Rows denote selector trained with α ; columns evaluate cost using α .

Policy	$\alpha = 0.2$	$\alpha = 0.5$	$\alpha = 0.8$
AUTO	0.510101	0.483153	0.456205
AUTO ($\alpha = 0.2$)	0.505359	0.480854	0.456348
AUTO ($\alpha = 0.5$)	0.506077	0.481263	0.456448
AUTO ($\alpha = 0.8$)	0.507218	0.480113	0.453008
GDSF	0.510865	0.481510	0.452155
LHD	0.521778	0.489596	0.457415
S3-FIFO	0.546445	0.517095	0.487745
SIEVE	0.529180	0.510413	0.491645
WTinyLFU-AV	0.552026	0.512398	0.472770

Table 15: AUTO vs SIEVE: cacheable-only OMR vs all-request BMR tradeoffs.

Case	Count	Fraction
OMR improves, BMR_all worsens	28	0.233
OMR worsens, BMR_all improves	6	0.050
Both improve	52	0.433
Both worsen	34	0.283

5.2 Per-workload wins

We report win counts on cacheable-only OMR (excluding degenerate trace-size pairs where policies are indistinguishable) in the reproducibility artifact. AUTO improves over SIEVE on most evaluated workloads (80/120 trace-size pairs) and beats S3-FIFO on 79/120 pairs with 22 ties. Against S3-FIFO, it wins in large-object regimes and mostly matches it in small-object regimes. When AUTO trails the best expert, a single policy typically dominates that trace across cache sizes, suggesting that pinning the expert is appropriate once the fingerprint consistently identifies that regime.

5.3 Trends across cache sizes

Figure 3 shows OMR/BMR as cache size increases for representative traces. The qualitative takeaway is that SCION avoids regime mismatch: it selects a size-aware expert on large-object traces and selects S3-FIFO on small-object traces.

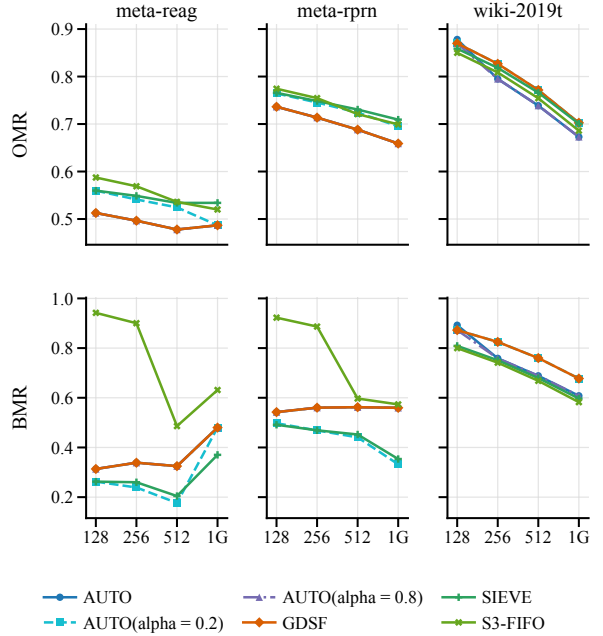


Figure 3: Cacheable-only OMR (top) and BMR (bottom) vs cache size for representative traces (lower is better for both).

5.4 Tail-window robustness

We analyze worst-5% window OMR/BMR across cache sizes as a simple tail proxy; artifact plots show that the wrong policy can incur large tail penalties.

Tail-aware selector. Using worst-5% window OMR as the training objective (on the subset of policies with per-window stats), we train a selector to directly target tail behavior. Tail-aware training reduces average/P95 tail regret from 0.0190/0.098 to 0.0116/0.073 (Table 16), suggesting that the fingerprint captures signal relevant to tail windows.

Table 16: Selector performance when trained on a tail objective (non-flat samples).

Objective	Acc \uparrow	Avg regret \downarrow	P95 regret \downarrow
OMR (subset)	0.592	0.019029	0.098285
Tail-5% OMR	0.625	0.011641	0.072579

AUTO vs fixed GDSF. GDSF remains the strongest average OMR baseline on this suite, while AUTO tends to trade small OMR losses for modest average BMR gains. For cacheable-only BMR, AUTO improves over GDSF on 20% of trace-size pairs with a mean

$\Delta = -0.0024$, aligning with the OMR/BMR tradeoff motivation. Full AUTO-GDSF deltas (max gap 0.14 OMR; incl. worst-5% windows) are in the reproducibility artifact.

Risk-sensitive regret. Table 17 reports mean, P90, and CVaR90 regret versus the best expert on cacheable-only OMR and BMR. On OMR, GDSF has lower mean and tail regret, while AUTO slightly reduces the worst-case regret. On BMR, AUTO lowers mean and tail regret relative to GDSF, matching the OMR/BMR tradeoff motivation. Per-trace regret CDFs and confidence-bucket breakdowns are included in the reproducibility artifact. Figure 4 gives a compact visual summary of two practical secondary results: the OMR/BMR regret tradeoff relative to fixed GDSF, and the fast-policy-budget operating point for AUTO-FAST.

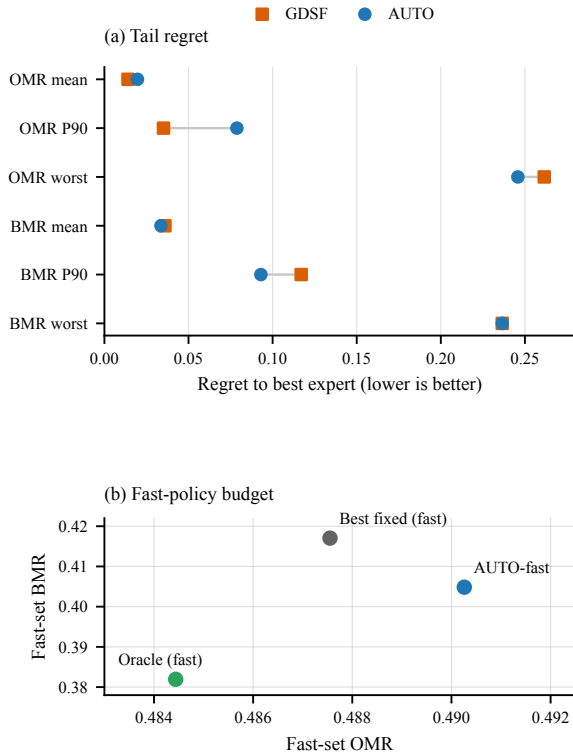


Figure 4: Two compact visual summaries of secondary analyses. Top: AUTO trades a small mean-OMR increase for better BMR tails and slightly lower worst-case OMR than fixed GDSF. Bottom: AUTO-fast improves the fast-budget Pareto point over the best fixed fast policy.

5.5 Sensitivity and nonstationarity

Prefix stability over time. Our main aggregate results use a single prefix-based selection for the full run.

Table 17: Risk-sensitive regret vs the best expert (cacheable-only).

Metric	Method	Mean regret	P90	CVaR90	Worst	N
OMR	AUTO	0.0197	0.0788	0.1265	0.2458	120
OMR	GDSF	0.0140	0.0351	0.1003	0.2615	120
BMR	AUTO	0.0336	0.0930	0.1508	0.2365	120
BMR	GDSF	0.0360	0.1170	0.1590	0.2365	120

To quantify how stable that choice remains, we evaluate cacheable-only OMR regret per 200k-request window relative to the per-window best expert, using the expert chosen by AUTO for that trace-size pair. Table 18 reports post-prefix windows (excluding the selection window): the median regret is 4.15×10^{-4} , 63.7% of windows are within 0.01 OMR, and 82.4% are within 0.05 OMR. However, the prefix-best expert remains best in only 52.9% of windows, indicating within-trace drift and motivating periodic re-selection when switching costs allow. In spliced traces, a low-switch fixed-share baseline ($\alpha = 0.05$) matches fixed GDSF within 0.0005 OMR on average (Table 22), suggesting that conservative re-selection can track drift without excessive oscillation. This window-level stability provides a proxy for prefix-placement sensitivity: even if the initial prefix is atypical, the selected expert remains close to the per-window best for most of the run. Operationally, the p90-threshold selector is already stable with $N = 1k-10k$ requests, and $N = 50k$ performs similarly to $N = 200k$ for the multi-feature selector (Table 21). We recommend choosing the smallest N for which p90, cacheable fraction, and unique ratio stop changing materially across consecutive windows; on this suite, that occurs by 1k-10k requests for SCION-P90 and by about 50k for the multi-feature selector. Re-select every N requests (or when change-points in these statistics or low-confidence spikes appear), trading switch cost for drift tracking.

Table 18: Prefix-based selection stability (post-prefix windows; cacheable-only OMR).

Metric	Value
Trace-size pairs	98
Post-prefix windows	2282
Median regret	0.000415
P90 regret	0.091308
Frac ≤ 0.01	0.637
Frac ≤ 0.02	0.702
Frac ≤ 0.05	0.824
Prefix-best stays best	0.529

Out-of-distribution generalization. We evaluate cross-family generalization by training on one dataset group and testing on another. As a temporal split within a single dataset, training on CloudPhysics weeks 01–02 and testing on weeks 03–04 yields accuracy 0.375 with avg regret 0.0259; the reverse split is harder (avg regret 0.0679), highlighting natural drift even without cross-domain shifts. Table 19 shows that training on non-Twitter traces transfers well to Twitter (acc 0.75, avg regret 6×10^{-6}), while Twitter-only training generalizes less well to non-Twitter workloads (acc 0.47, avg regret 0.0176). Block traces are moderately harder out-of-distribution (avg regret 0.0208 when trained on non-block traces), underscoring the need for diverse training traces and richer fingerprints when deploying a fixed offline selector.

Cache-size generalization. Holding out one cache size at a time (train on three sizes, test on the fourth) yields 0.57–0.67 accuracy with average regret 0.014–0.022 on the held-out size, suggesting reasonable within-range generalization (artifact table). To test true extrapolation, we additionally ran four traces at 64 MiB and 2 GiB, outside the 128 MiB–1 GiB training range: average regret rises to 0.029 and AUTO trails GDSF by 0.022 OMR on average, with the largest miss concentrated on CloudPhysics-w01. In practice, deployments far outside the training range should retrain or include representative sizes in the selector’s training set.

Table 19: Out-of-distribution generalization by dataset family (OMR objective).

Train - i Test	Acc	Avg regret	P95 regret	N
non-twitter - i twitter	0.750	0.000006	0.000023	24
twitter - i non-twitter	0.469	0.017631	0.078119	96
non-block - i block	0.521	0.020802	0.101020	48
block - i non-block	0.319	0.008301	0.041023	72
cloudphysics early - i cloudphysics late	0.375	0.025894	0.053132	8
cloudphysics late - i cloudphysics early	0.375	0.067903	0.147991	8

Table 20 reports a compact sensitivity summary over N and τ , including alternative fingerprints. We find that percentile-based fingerprints (p90) reduce regret relative to the mean under heavy-tailed sizes. Notably, the best p90 setting already uses $N=1k$ – $10k$ requests, indicating that very short prefixes can be sufficient for selection. Table 21 summarizes p90-threshold performance across prefix lengths (best τ per N); regret is essentially unchanged from $N=1k$ to $N=200k$ on this trace suite, suggesting that very short prefixes can drive the cheap threshold selector; at $N=50k$ the regret matches the

$N=200k$ setting (Table 21). Table 22 evaluates online epochal selection on spliced traces (large→small and small→large), including hysteresis (lag/min-stay) and window-level bandit baselines (epsilon-greedy, Hedge, and EXP3; LeCaR-style online expert tracking); infrequent re-selection can track regime changes with limited degradation. These spliced experiments switch experts without state transfer (cold-start), which upper-bounds practical switching cost when warm transitions or shadowing are used in systems; our prototype warm-switch recovers up to 3 percentage points of hit ratio (artifact). We additionally include a fixed-share (tracking) meta-algorithm with switching-cost awareness and an offline switching-cost oracle to contextualize online performance under regime changes. We model switching cost as an additive 2% miss penalty per switch in these simulations (switch counts are summarized in the reproducibility artifact). These serve as empirical reference points; we do not derive formal tracking or switching-cost guarantees in this work. The full per-trace spliced results are in the reproducibility artifact. Average switch counts show that the threshold and fixed-share selectors switch only a handful of times per run, while bandit/EXP3-style baselines switch far more frequently.

Table 20: Fingerprint sensitivity (best setting per fingerprint across N and τ).

Fingerprint	N	τ (bytes)	Miscs	Avg regret	Worst regret
logmean	1000	262144	0.742	0.036269	0.542588
mean	1000	262144	0.608	0.031072	0.542588
median	1000	262144	0.708	0.036070	0.542588
p90	1000	262144	0.475	0.025470	0.542588
trimmed	5000	262144	0.608	0.031072	0.542588

Table 21: Short-prefix p90 threshold sensitivity (best τ per N).

Prefix N	Best τ	Avg regret	P95 regret ↓
1K	256KiB	0.025470	0.029927
5K	256KiB	0.026814	0.031231
10K	256KiB	0.026814	0.031231
50K	256KiB	0.026814	0.031231
200K	256KiB	0.026814	0.031231
1M	256KiB	0.027014	0.031437

5.6 Synthetic stress tests

To probe extreme regimes not well represented in public traces, we generate synthetic oracleGeneral traces with

Table 22: Online epochal selection on spliced traces (summary; cacheable-only OMR).

Mode	Avg OMR ↓	Best OMR ↓	Worst OMR ↓
oracle_switch(cost=0.02)	0.566952	0.477694	0.647771
fixed_share(alpha=0.05)	0.569891	0.478663	0.652027
fixed:GDSF	0.570428	0.477694	0.654674
hedge	0.571376	0.478663	0.655083
threshold	0.571516	0.479902	0.654131
bandit	0.587959	0.494979	0.694912
fixed:SIEVE	0.595822	0.500604	0.676335
exp3	0.604616	0.505300	0.686499
fixed:S3-FIFO	0.607712	0.504683	0.691214

(i) very high hotspots (Zipf $\theta=1.1$), (ii) high-churn/near-write-dominated streams (95% unique ratio), and (iii) rapid regime switches (hotspot→uniform). We report cacheable-only OMR/BMR at 256 MiB over 1M requests per synthetic trace. Table 23 (cells show OMR/BMR) indicates that the same regime split persists: size-aware policies dominate large-object regimes, while FIFO-family policies dominate small-object regimes; SCION-P90 avoids the worst mismatches.

Table 23: Synthetic stress tests (cacheable-only OMR/BMR at 256 MiB, 1M requests).

Trace	S3-FIFO	GDSF	SIEVE	ARC	SCION-P90
Hotspot (Zipf 1.1), large objects	0.472/0.470	0.389/0.388	0.508/0.507	0.492/0.490	0.389/0.388
Hotspot (Zipf 1.1), small objects	0.155/0.154	0.136/0.135	0.155/0.154	0.150/0.149	0.155/0.154
High churn (95Regime switch (hotspot→uniform))	0.668/0.475	0.527/0.393	0.740/0.507	0.683/0.525	0.527/0.393

5.7 Overhead-aware budget

To connect throughput overheads to operator decisions, we define a fast-policy budget using median MQPS from Table 25: policies with MQPS ≥ 4.5 (SIEVE, S3-FIFO, LHD, AdaptiveClimb, DynamicAdaptiveClimb). We retrain the selector on this restricted set (AUTO-fast) and compare against the best fixed fast policy and the per-trace oracle. AUTO-fast is trained on the same $\alpha=0.5$ cost objective used in Table 14 (within the fast set). Table 24 shows that AUTO-fast trades a small OMR increase for a larger BMR reduction; under the $\alpha=0.5$ cost objective used for training, this yields a lower average cost than the best fixed fast policy (LHD). The oracle row quantifies remaining headroom. This illustrates how SCION can incorporate CPU budgets by constraining or reweighting the expert set. Because these budgets depend on `libCacheSim` implementations, production-grade TinyLFU variants (e.g., Caffeine/Ristretto) could shift the fast set; we did not benchmark them here, but

the same MQPS-driven filter would apply. Accordingly, the 4.5 MQPS threshold should be read as a simulator-specific screening rule, not a universal deployment constant. Given Table 25, WTinyLFU-AV would require roughly a $100\times$ speedup to meet the 4.5 MQPS fast-set threshold. As a sensitivity check, if WTinyLFU-AV were fast enough to qualify, the fast-set oracle would improve by ≈ 0.008 OMR and ≈ 0.014 BMR (cacheable-only averages); we do not retrain AUTO-fast under this assumption.

Table 24: Overhead-aware selection under a fast-policy budget (cacheable-only averages).

Selector	Policy	Avg OMR ↓	Avg BMR ↓
Best fixed (fast)	LHD	0.487550	0.417048
AUTO-fast	AUTO-fast	0.490259	0.404845
Oracle (fast)	oracle	0.484438	0.381937

5.8 Overheads

Fingerprint cost. Computing the 200k-request prefix fingerprint takes about 1.6s on our CPU-only setup (median across traces), and runs once per epoch/window rather than on the hot path. Across 10 smaller traces (1M requests, 200k-request windows), the median per-window fingerprint cost is 1.64s (p90 1.70s), equivalent to $\approx 8\mu\text{s}$ per request when amortized, or $\approx 8.2\text{s}$ of background CPU time per 1M requests. We provide a script to reproduce these cumulative epoch-level measurements.

Per-policy throughput. Table 25 reports single-threaded throughput for representative policies. Queue-based FIFO-family policies are fastest; GDSF is slower due to priority-queue updates, and W-TinyLFU-AV incurs substantial overhead from its admission sketch. AdaptiveClimb/DynamicAdaptiveClimb are comparable to SIEVE. S3-FIFO in `libCacheSim` maintains multiple queues and a ghost list and is not heavily optimized, which can depress throughput; production implementations may differ. Our W-TinyLFU-AV implementation is the `libCacheSim` research version; production-grade TinyLFU deployments (e.g., Caffeine, Ristretto) are heavily optimized and can have materially higher throughput [15, 13]. Accordingly, we treat MQPS as an implementation-level overhead indicator rather than an algorithmic guarantee and avoid over-interpreting cross-policy throughput rankings. We do not yet proxy production admission paths in our harness; integrating those variants is future work that could refine the fast-policy budget results.

Table 25: Per-policy throughput microbenchmark.

Policy	Avg MQPS	Rel. to SIEVE
SIEVE	8.520	1.00x
AdaptiveClimb	8.512	1.00x
DynamicAdaptiveClimb	8.188	0.96x
S3-FIFO	5.708	0.67x
LHD	4.945	0.58x
GDSF	2.738	0.32x
WTinyLFU-AV	0.047	0.01x

5.9 End-to-end prototype

Table 26 summarizes the real-system prototype using 20k-request prefixes per trace. Even with a lightweight implementation, the same regime split is visible: AUTO selects the appropriate expert and reduces origin traffic while maintaining good latency and throughput, including against SIEVE. The prototype uses SCION-P90 (no offline training); in the full simulator, SCION-P90 trails AUTO by 0.0205 OMR and 0.0062 BMR on average (artifact table), so the prototype remains representative of the learned selector’s regime choices.

Switching-cost microbenchmark. We approximate the operational cost of switching experts by splitting a 20k-request trace into two halves and comparing *warm* (shadow-cache) versus cold switches. A warm switch recovers up to 3 percentage points of hit ratio versus cold-start (details in the artifact), so the spliced-trace results that assume cold-start are conservative for deployments that can warm transitions.

6 Discussion and Outlook

Interpretation. The result is not that a new policy beats all baselines everywhere; rather, the orchestration layer helps avoid regime mismatches when the operator objective is multi-dimensional (OMR vs BMR) or subject to CPU budgets. In workloads where a baseline is already optimal (e.g., small-object regimes for S3-FIFO), the right behavior is to select it. This tradeoff- and overhead-focused goal aligns with the direction of recent learned caching work [20, 23, 29]. Accordingly, AUTO is positioned as a pragmatic default for heterogeneous deployments, not as a universal winner on any single average metric. We do not introduce a new replacement algorithm; learning is used only to select among existing experts off the hot path. Practically, CloudPhysics-like traces and any deployment with persistent high fallback or a single-expert winner across sizes are “do not orchestrate” cases where pinning GDSF/S3-FIFO is preferable.

What this does *not* solve yet. Our prototype uses a small expert set and a tiny feature vector, but still stops short of full online selection with delayed feedback and does not yet optimize tail-latency proxies. The end-to-end prototype is intentionally minimal: it omits TTLs, revalidation, invalidations, and distributed consistency, which are important in production caches but orthogonal to the selection mechanism studied here. We also do not yet report full-trace results for every classic or cost-aware policy (e.g., ARC/LIRS/TwoQ, CAMP) or production-grade TinyLFU implementations across all sizes; the harness supports many of these, and expanding that coverage is straightforward but compute-intensive. Our main sweep covers 128–1024 MiB. The 64 MiB/2 GiB spot-check above suggests within-range generalization is materially better than true extrapolation, so deployments far outside that range should retrain or include those sizes; broader normalized C /working-set analyses remain future work. Finally, our confidence score is a coarse margin; it is not calibrated, and fallback defaults to GDSF in our experiments.

Switching costs (prototype view). Our prefix-stability analysis shows that some degree of drift is common even when median regret is small. The microbenchmark above suggests that simple shadow-cache warmup can reduce switching penalties; full production costs remain future work.

7 Related Work

Learned caching for systems. LRB [19] and Cacheus [16] explore learned admission/replacement and mixtures of experts; Cacheus maintains per-request mixture weights, whereas SCION selects per-trace/epoch based on a tiny fingerprint. This decoupling enables explicit reject-option fallback and throughput budgeting without per-request ML. Recent work emphasizes deployability and low overhead (e.g., HALP, MAT, and 3L-Cache) [20, 23, 29]. We compare to Cacheus/LeCaR on a small subset due to harness cost; HALP/MAT/3L-Cache implementations are not available in `libCacheSim` and place ML on the hot path, so we treat them as complementary and discuss their overhead relative to our fast-policy budget. Unlike these methods, SCION keeps inference entirely off the hot path and only selects among existing experts, trading potential algorithmic optimality for operational simplicity and robustness. HR-Cache [21], Cold-RL [10], and LCR/LARU [8] instead keep learning on the hot path while targeting BMR or bounded overhead.

TTL-based admission and expiration. TTL policies control admission and eviction using per-object time-to-live values, with adaptive variants such as d-TTL and

Table 26: End-to-end prototype results (cache-daemon + origin).

Trace	Policy	Cache	P50 ms	P95 ms	P99 ms	RPS	Hit	Origin GB
meta_reag.oracleGeneral.zst	SIEVE	256MiB	46.62	3023.18	8214.08	128.5	0.319	290.87
meta_reag.oracleGeneral.zst	GDSF	256MiB	41.96	3035.64	8774.38	128.8	0.365	298.09
meta_reag.oracleGeneral.zst	AUTO	256MiB	43.74	3162.16	8368.71	123.6	0.364	296.03
meta_reag.oracleGeneral.zst	S3-FIFO	256MiB	48.36	3038.00	7871.37	120.2	0.317	291.14
meta_rprn.oracleGeneral.zst	GDSF	256MiB	53.49	1358.30	4809.51	73.0	0.240	648.03
meta_rprn.oracleGeneral.zst	S3-FIFO	256MiB	46.94	1170.62	3870.59	71.7	0.206	647.41
meta_rprn.oracleGeneral.zst	SIEVE	256MiB	48.39	1212.44	4285.68	74.1	0.206	647.65
meta_rprn.oracleGeneral.zst	AUTO	256MiB	47.34	1233.02	4134.08	73.5	0.239	647.92
wiki_2019t.oracleGeneral.zst	GDSF	256MiB	9.39	11.23	14.31	13598.2	0.119	0.59
wiki_2019t.oracleGeneral.zst	S3-FIFO	256MiB	10.47	29.04	31.18	8376.1	0.114	0.58
wiki_2019t.oracleGeneral.zst	SIEVE	256MiB	9.00	10.39	16.24	14220.0	0.111	0.59
wiki_2019t.oracleGeneral.zst	AUTO	256MiB	10.59	28.66	31.03	8439.4	0.114	0.58

f-TTL that tune TTLs to hit-rate or cache-size objectives under nonstationary demand [1]. These methods are complementary to SCION; TTL rules can act as experts or as admission filters upstream of replacement.

Online selection and no-regret caching. Regret-minimizing approaches such as LeCaR [22] and recent online gradient-based caching with logarithmic complexity [6] provide theoretical guarantees under adversarial or nonstationary sequences. SCION targets a different point in the design space: infrequent, off-path selection among a small expert set with minimal runtime state. For online expert tracking, fixed-share and related algorithms provide regret bounds against the best switching sequence [11, 7]; we include such baselines in our spliced-trace analysis.

Offline bounds and headroom. For variable-size caching, Belady is only one offline reference point. FOO/PFOO formulate tighter offline bounds via min-cost flow and quantify remaining OPT headroom under variable object sizes [4]. Our Belady/BeladySize subset should therefore be read as a lightweight oracle sanity check, not as the last word on offline headroom.

Learning for replacement (broader contexts). Imitation-learning and “approximate MIN” approaches (e.g., Parrot; Hawkeye/OPTgen) aim to mimic Belady-style decisions [14, 12]. Other learned replacement work explores RL-derived policies and reuse-distance prediction (e.g., RLR, Mockingjay) [17, 18]. These lines inform SCION’s ethos: use learning to *select* or *approximate* what is hard, while keeping the online path simple.

Strong non-ML object caching. SIEVE and S3-FIFO are recent strong baselines [28, 26]; classic size-aware scoring (GDS/GDSF) remains effective in large-object regimes [5], and benefit/density-based heuristics such as LHD have been studied for object caches [2]. AdaptiveClimb and DynamicAdaptiveClimb offer low-overhead alternatives with strong performance across diverse traces [3]. Clock2Q+ extends queue-based designs for metadata caches and reports strong low-overhead performance [27]; its target workload is storage metadata rather than variable-size CDN/object traces, so we treat it as a future expert candidate rather than a direct baseline here. Cost-aware approximations to GDS and production-grade TinyLFU variants (e.g., Caffeine/Ristretto-style implementations) are natural expert candidates for SCION [15, 13].

8 Conclusion

We presented SCION, a lightweight orchestration framework for object-cache replacement policies. The main result is not that AUTO dominates every expert on average; it is that a tiny off-path fingerprint is often enough to automate policy choice, expose explicit OMR/BMR/CPU tradeoffs, and identify when operators should pin a single expert instead. Across public traces and synthetic stress tests, the main regime split is size-aware vs FIFO-family, while the remaining oracle gap is more pronounced for byte-aware objectives than for OMR. We provide a reproducible benchmark, selector training pipeline, and prototype; future work will add richer offline bounds, production-grade fast baselines, and fuller online switching.

References

- [1] S. Basu, A. Sundarrajan, J. Ghaderi, S. Shakkottai, and R. Sitaraman. Adaptive TTL-based caching for content delivery. *IEEE/ACM Transactions on Networking*, 26(3):1063–1077, June 2018.
- [2] N. Beckmann, H. Chen, and A. Cidon. LHD: Improving cache hit rate by maximizing hit density. In *15th USENIX Symposium on Networked Systems Design and Implementation (NSDI 18)*, pages 389–403, Renton, WA, USA, Apr. 2018. USENIX Association.
- [3] D. Berend, S. Dolev, S. Kumari, D. Mishra, M. Kogan-Sadetsky, and A. Somani. Dynamicadaptiveclimb: Adaptive cache replacement with dynamic resizing. arXiv preprint arXiv:2511.21235, 2025.
- [4] D. S. Berger, N. Beckmann, and M. Harchol-Balter. Practical bounds on optimal caching with variable object sizes. *Proc. ACM Meas. Anal. Comput. Syst.*, 2(2), June 2018.
- [5] P. Cao and S. Irani. Cost-aware WWW proxy caching algorithms. In *Proceedings of the USENIX Symposium on Internet Technologies and Systems*, Monterey, CA, USA, Dec. 1997. USENIX Association. Introduces GreedyDual-Size (GDS) family; GDSF is a common frequency-augmented variant.
- [6] D. Carra, G. Neglia, and X. Zhang. Low-complexity online learning for caching. *Computer Networks*, 273, Dec. 2025.
- [7] N. Cesa-Bianchi and G. Lugosi. *Prediction, Learning, and Games*. Cambridge University Press, Cambridge, UK, 2006.
- [8] P. Chen, J. Zhang, H. Zhao, Y. Zhang, J. Yu, X. Tang, Y. Wang, H. Li, J. Zou, G. Xiong, K. Chow, S. He, and S. Deng. Toward robust and efficient ML-based GPU caching for modern inference. arXiv preprint arXiv:2509.20979, 2025. Introduces LCR/LARU.
- [9] G. Einziger and R. Friedman. TinyLFU: A highly efficient cache admission policy. In *22nd Euromicro International Conference on Parallel, Distributed, and Network-Based Processing, PDP 2014, Torino, Italy, February 12-14, 2014*, pages 146–153. IEEE Computer Society, 2014.
- [10] A. Gupta and A. Bhayani. Cold-rl: Learning cache eviction with offline reinforcement learning for NG-INX. arXiv preprint arXiv:2508.12485, 2025.
- [11] M. Herbster and M. K. Warmuth. Tracking the best expert. *Machine Learning*, 32(2):151–178, Aug. 1998.
- [12] A. Jain and C. Lin. Back to the future: Leveraging belady’s algorithm for improved cache replacement. In *43rd ACM/IEEE Annual International Symposium on Computer Architecture, ISCA 2016, Seoul, South Korea, June 18-22, 2016*, pages 78–89. IEEE Computer Society, 2016.
- [13] D. Labs. Ristretto: A high performance memory-bound Go cache. <https://github.com/hypermodeinc/ristretto>. Accessed 2026-03-21.
- [14] E. Z. Liu, M. Hashemi, K. Swersky, P. Ranganathan, and J. Ahn. An imitation learning approach for cache replacement. In *Proceedings of the 37th International Conference on Machine Learning*, volume 119 of *Proceedings of Machine Learning Research*, pages 6237–6247. PMLR, July 2020.
- [15] B. Manes. Caffeine: A high performance caching library for Java. <https://github.com/ben-manes/caffeine>. Accessed 2026-03-21.
- [16] L. V. Rodriguez, F. Yusuf, S. Lyons, E. Paz, R. Rangaswami, J. Liu, M. Zhao, and G. Narasimhan. Learning cache replacement with CACHEUS. In *19th USENIX Conference on File and Storage Technologies (FAST 21)*, pages 341–354. USENIX Association, Feb. 2021.
- [17] S. Sethumurugan, J. Yin, and J. Sartori. Designing a cost-effective cache replacement policy using machine learning. In *IEEE International Symposium on High-Performance Computer Architecture, HPCA 2021, Seoul, South Korea, February 27 - March 3, 2021*, pages 291–303. IEEE, 2021.
- [18] I. Shah, A. Jain, and C. Lin. Effective mimicry of belady’s MIN policy. In *International Symposium on High-Performance Computer Architecture*, pages 558–572, 2022.
- [19] Z. Song, D. S. Berger, K. Li, and W. Lloyd. Learning relaxed belady for content distribution network caching. In *17th USENIX Symposium on Networked Systems Design and Implementation (NSDI 20)*, pages 529–544, Santa Clara, CA, USA, Feb. 2020. USENIX Association.
- [20] Z. Song, K. Chen, N. Sarda, D. Altınbüken, E. Brevdo, J. Coleman, X. Ju, P. Jurczyk, R. Schooler, and R. Gummadi. HALP: Heuristic aided learned preference eviction policy for YouTube content delivery network. In *20th USENIX Symposium on Networked Systems Design and Implementation (NSDI 23)*, pages 1149–1163, Boston, MA, USA, Apr. 2023. USENIX Association.

- [21] H. Torabi, H. Khazaei, and M. Litoiu. A learning-based caching mechanism for edge content delivery. In *Proceedings of the 15th ACM/SPEC International Conference on Performance Engineering (ICPE '24)*, London, United Kingdom, May 2024. ACM.
- [22] G. Vietri, L. V. Rodriguez, W. A. Martinez, S. Lyons, J. Liu, R. Rangaswami, M. Zhao, and G. Narasimhan. Driving cache replacement with ML-based LeCaR. In *10th USENIX Workshop on Hot Topics in Storage and File Systems (HotStorage 18)*, Boston, MA, USA, July 2018. USENIX Association.
- [23] D. Yang, D. S. Berger, K. Li, and W. Lloyd. A learned cache eviction framework with minimal overhead. arXiv preprint arXiv:2301.11886, 2023.
- [24] J. Yang. libcachesim. <https://github.com/cacheMon/libCacheSim>. Accessed 2026-03-21.
- [25] J. Yang. cache_dataset: A public cache trace dataset and tools. https://github.com/cacheMon/cache_dataset, 2024. Accessed 2026-03-21.
- [26] J. Yang, Y. Zhang, Z. Qiu, Y. Yue, and R. Vinayak. FIFO queues are all you need for cache eviction. In *Proceedings of the 29th Symposium on Operating Systems Principles, SOSP 2023, Koblenz, Germany, October 23-26, 2023*, pages 130–149. ACM, 2023.
- [27] Y. Zhai, B. D. Marthen, S. Balivada, V. S. Bojji, E. Knauft, J. Rohilla, J. Zuo, Q. Liu, M. Austruy, W. Wang, and J. Yang. Clock2q+: A simple and efficient replacement algorithm for metadata cache in VMware vSAN. arXiv preprint arXiv:2511.21958, 2025.
- [28] Y. Zhang, J. Yang, and A. Awad. SIEVE is simpler than LRU: An efficient turn-key eviction algorithm for web caches. In *Proceedings of the 21st USENIX Symposium on Networked Systems Design and Implementation (NSDI 24)*, pages 487–503, Santa Clara, CA, USA, Apr. 2024. USENIX Association.
- [29] W. Zhou, Z. Niu, Y. Xiong, J. Fang, and Q. Wang. 3L-Cache: Low overhead and precise learning-based eviction policy for caches. In *23rd USENIX Conference on File and Storage Technologies (FAST 25)*, pages 237–254, Santa Clara, CA, USA, Feb. 2025. USENIX Association.